Crustal and Upper Mantle Structure of the Solomon Islands as Revealed by Seismic Refraction Survey of November–December 1966[1]

A. S. FURUMOTO, D. M. HUSSONG, J. F. CAMPBELL, G. H. SUTTON, A. MALAHOFF, J. C. ROSE, and G. P. WOOLLARD[2]

ABSTRACT: A seismic refraction survey was carried out in the waters around the Solomon Islands during November and December 1966. Three ships were involved in the survey: two, stationed at the end points of the traverses, acted as recording ships; the third steamed along the traverses and dropped explosives. Reflection profiling and magnetic surveys were simultaneously carried out with the refraction survey. The results show that (a) on the Ontong Java Plateau to the northwest of the islands the crust is about 25 km thick with subnormal crustal velocities; (b) southwest of the New Georgia Islands the crust is thinner than normal and is underlain by a mantle with low velocity; (c) southwest of Bougainville Island the crust is generally of normal oceanic structure underlain by a mantle with low velocity; and (d) mantle material in the Slot is found at a depth of 14 km.

IN NOVEMBER AND DECEMBER 1966, members of the Hawaii Institute of Geophysics carried out a series of twelve marine seismic refraction traverses in the Solomon Islands area. Two recording ships held station at opposite ends of each of the refraction lines and a third ship fired charges between the two. Magnetic and seismic (sparker) reflection profiling measurements were also carried out in conjunction with the refraction measurements. Only the refraction results are reported here.

The objective of the refraction study was to determine the degree to which the unusual gravity anomalies recorded in the Solomon Islands Archipelago reflect the crustal and upper mantle composition and structure. Orbital perturbations of the paths of artificial satellites traversing the region—which indicated a pronounced rise in the geoid—led to land gravity surveys of the Solomon Islands and the adjacent Bismarck Archipelago and New Guinea from 1963 to 1965, subsequently reported by Laudon (1968) and Grover (1968), and to a gravity survey of the adjacent sea area, reported by Rose, Woollard, and Malahoff (1968). The marine gravity survey, in particular, showed that deep-water areas in the Coral Sea to the south of the Solomon Islands were characterized by very high (+100 mgal) positive free-air anomalies.

Grover (1968), in interpreting the results, found a correlation of the land gravity values with surface geological features. Rose, Woollard, and Malahoff (1968) showed that the gravity anomalies could be used to obtain estimates of crustal thickness in the region. These estimates are in substantial agreement with the seismic refraction values reported here.

FIELD OPERATION

In laying out the traverses for the seismic refraction measurements, the investigators were guided by the free-air gravity anomaly pattern show in Figure 1 and the bathymetry as shown in Figure 2. The anomaly relations to depth of water were normal at about half the sites and abnormal for the other half. Lines A, B, and C, north of the Solomon Islands, are in an area of predominantly negative free-air anomalies where sparker measurements (Woollard et al., 1967) show there is both an apparent crustal arch and a trench. Line P is in the Slot between the northern and southern series of islands where the free-air anomalies are essentially zero; Line D, south of Guadalcanal, is where there is a trench and the free-air anomalies are

[1] Hawaii Institute of Geophysics Contribution No. 337. Manuscript received September 26, 1969.

[2] Hawaii Institute of Geophysics, University of Hawaii, Honolulu 96822.

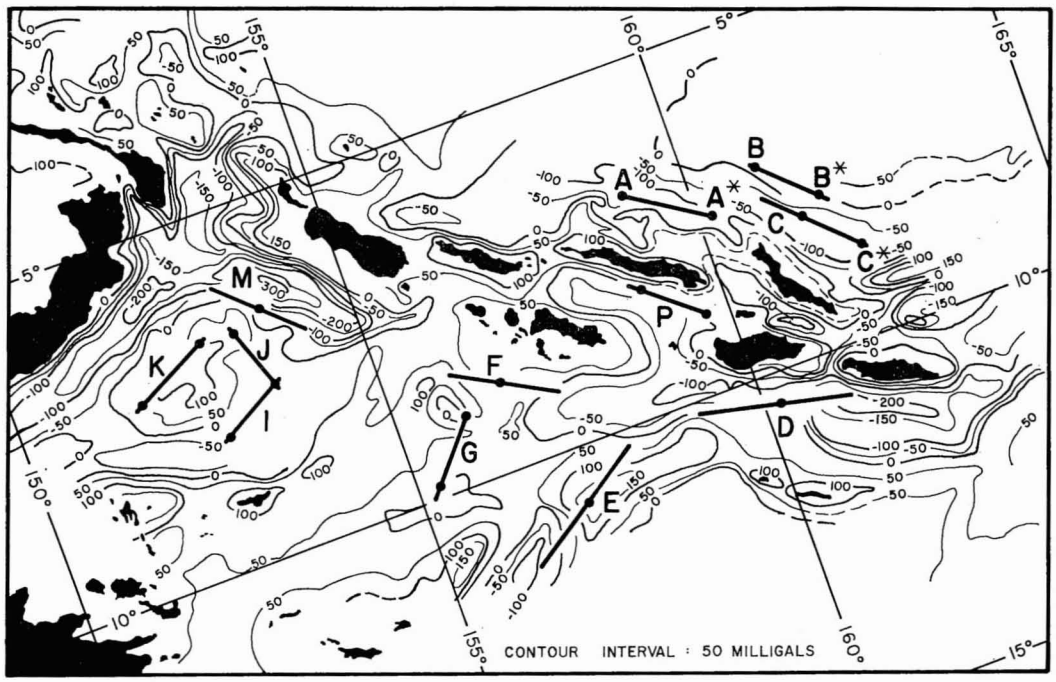

FIG. 1. Free-air gravity anomaly map of the Solomon Islands area showing the locations of seismic refraction traverses. Free-air gravity anomaly contour intervals: 50 milligals.

negative; Line E is where there is a rise in the sea floor and a positive gravity anomaly; Line F is in a trench area characterized by positive free-air anomalies; Line G is on a bathymetric rise characterized by positive gravity anomalies; Line M is over the deep (—8 km) Bougainville Trench where the free-air anomalies are over — 300 mgal; and lines J, K, and I are in a deep-water (—4 km) area where the free-air anomalies reach +100 mgal. No attempt was made to conduct land-based refraction measurements because of the rugged jungle terrain and inaccessibility of the interior of the islands. Nearshore measurements were ruled out by the numerous uncharted reefs which make navigation in these waters hazardous. As the thickness of the crust deduced from the gravity data was of the order of about 20 km, the refraction lines were planned to probe to at least that depth.

Three ships were used in carrying out the refraction program. The largest, the SS "Taranui" (700 tons), was used as the shooting ship, while the two smaller vessels, MV "California" and RV "Machias," diesel-powered auxiliary sailing vessels, were used as recording ships. The "Taranui" also carried out the magnetic surveys and seismic reflection profiling measurements.

The seismic recording instrumentation was similar to the system described by Shor (1963). A tape recorder, which was tried in place of a photographic recorder, proved to be unsatisfactory. For the greater part of the field work, the seismic arrivals were received on visual recorders.

In carrying out the measurements, the recording vessels were positioned about 90 km apart at the opposite ends of the traverse. The "Taranui" then made a run between the two, dropping explosive charges along the way. The charges varied from 1 pound to 200 pounds of nitramon WWEL and were detonated by the lit-fuse method. The shooting vessel monitored and transmitted the detonation time by radio to the recording vessels.

The traverses were carried out in alphabetical sequence except for Line F, which was passed over and done later because of instrumental difficulties encountered aboard the recording vessel "California." Because of earlier instru-

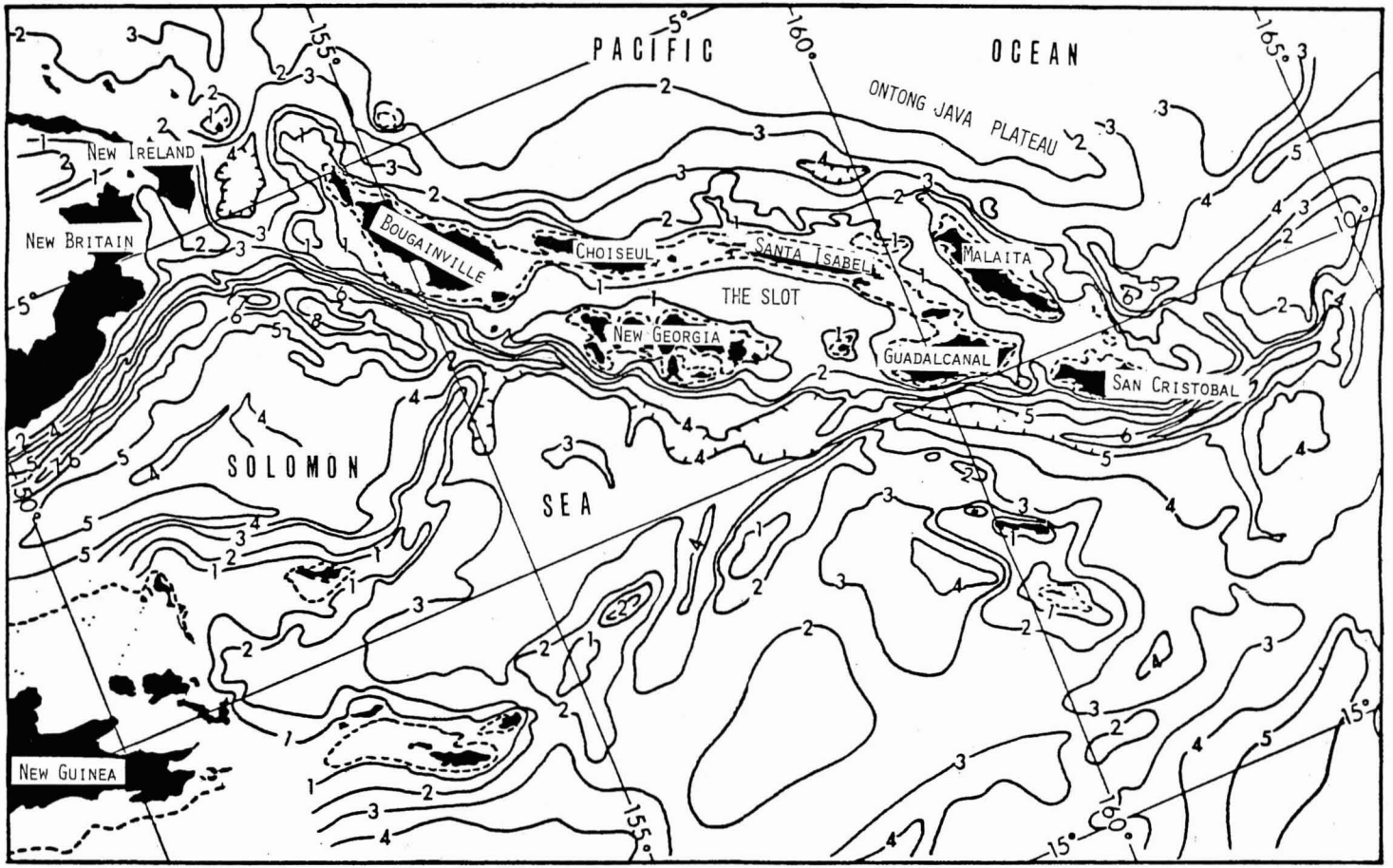

FIG. 2. Bathymetry of the Solomon Islands area. Depth contours are in kilometers.

TABLE 1

LOCATION OF SEISMIC REFRACTION TRAVERSES IN THE SOLOMON SEA AREA

LINE	MV "CALIFORNIA" POSITION		RV "MACHIAS" POSITION		REMARKS
	LAT. S	LONG. E.	LAT. S	LONG. E.	
A			6°52′	159°25′	Reversed by two single-ended profiles
A*			7°32′	160°10′	
B			7°06.5′	161°00′	Reversed by two single-ended profiles
B*			7°48.5′	161°44′	
C			8°00′	161°22′	Reversed by two single-ended profiles
C*			8°41.5′	162°06′	
D			10°27′	160°15′	Split profile, azimuth 282°
E			10°49′	157°13′	Split profile, azimuth 55°
F			8°44′	156°37′	Split profile, azimuth 118°
G	9°04′	155°57′	9°50′	155°18′	Reversed
I	7°37′	153°38′	8°06′	152°45′	Reversed
J	7°37′	153°38′	6°45′	153°18′	Single-ended
K	6°42′	152°48′	7°15′	151°45′	Reversed
M			6°31′	153°45′	Split profile, azimuth 133°
P	8°51′	159°41′	8°12′	158°54′	Reversed

mentation problems, lines A, B, and C were first shot as single-ended profiles. After completion of the other lines, a second phase of the project "reversed" profiles A, B, and C by shooting them with a recording ship on opposite ends of the lines. Lines D, E, M, and F were shot as split profiles. Line J was attempted as a reversed profile, but instrumental difficulties on the eastern end in effect made it a single-ended profile. The rest of the profiles were reversed.

The location and the description of the measurements at each site are listed in Table 1. A detailed cruise report of the expedition has already been published (Woollard et al., 1967).

THE OBSERVED TRAVEL-TIME PLOTS AND DERIVED CRUSTAL SECTION

The quality of the data varied from line to line but on the whole can be classified as fair to good. The principal defect in the data lies in the lack of good first arrivals for the mantle where the crustal thickness was of the order of 20 km. For most of the traverses, the direct water-wave arrival from the detonation was clearly recorded, and the water-wave travel time was used to determine the shot distances. When the direct water-wave signal began to fade, equivalent arrival times for the direct water-wave were obtained by applying corrections to the first bottom-reflected wave. Distances from the shot point to the recorder were calculated by multiplying the travel-time of the direct water-wave by 1.54 km/sec as defined by sea-water temperature and salinity values in the area.

On most traverses, the bottom topography was so variable that corrections for changes in water depth had to be applied to the seismic-wave arrival times. In those cases a straight base line was determined for each traverse, and corrections were calculated for deviations from this line using the method of Sutton and Bentley (1953).

The velocity-depth profiles defining crustal structure were calculated from the travel-time curves using the standard zero distance intercept method and assuming discrete layers having a constant velocity and plane boundaries. Admittedly, other interpretations of the data are possible, and, in fact, several interpretations of the data were made for each traverse. Only those considered to represent a best fit to the data are presented here.

The time-intercept and velocity values for each layer defined at each site are tabulated in Table 2. The derived thickness of each layer and its velocity are tabulated in Table 3. The layers have been arbitrarily named a, b, c, and d—based on similarity of velocity values.

LINES A–A*, B–B*, AND C–C*: As has been mentioned, lines A–A*, B–B*, and C–C* all lie north of the island chain. Although in each case these traverses represent two single-ended profiles, they are in effect reversed profiles. However, they are not true reverses because navigational difficulties made it impossible to have the second positions of the series of observations coincide exactly with those for the first series. Because of this limitation the various branches of the travel-time plots for the single-ended profiles were paired off primarily on the basis of similarity of velocity values.

The travel-time plots for Lines A–A* and B–B* are shown in Figure 3. In Line A–A*, although there were only a few first arrivals from the mantle, the velocity appears to be fairly well established as about 8.0 km/sec. Arrivals from the crustal layers are in good agreement for the two series of measurements except for the upper crustal layer (4.6 versus 3.8 km /sec). For the B series of observations, no mantle arrival can be identified, and on Line B* the mantle is defined only by second arrivals out to a distance corresponding to a direct water-wave travel-time of 90 seconds. Even if the use of second arrivals is questioned, it can be safely said that the crust is thicker than 20 km.

The travel-time plots for Lines C and C* are shown in Figure 4. Both define a high-velocity basal layer in the crust having a value of 7.0 to 7.1 km/sec—although the layer is not evident on profiles A–A* and B–B*. The mantle velocity is defined on profile C but not on C*. It is high (8.5 km/sec). In computing the mantle depth under site C, the Moho discontinuity was assumed to be horizontal, and the mantle velocity obtained (8.5 km/sec) was used, although this velocity value may be too high. Figure 5 compares the derived crustal sections for each site. The thickest crust (site B) is on the Ontong Java Plateau where sparker measurements (Woollard et al., 1967) show there is a pronounced crustal arch. The refraction results suggest that this flexure is related to a thickening of the basal (6.2 km/sec) layer.

The crustal thickness for site C is abnormally large for the water depth of +3,000 meters, and the mean crustal velocity is markedly abnormal relative to that for sites A and B. The mantle velocity (8.5 km/sec) is also abnormal. The abnormalities are similar to those noted by Woollard (1968) for continents where a direct relationship is found between abnormality in crustal velocity, crustal thickness, and mantle velocity.

LINES D AND E: The travel-time plots for Lines D and E are shown in Figure 6. In Line D, the velocity structure defined for the crust is intermediate between that defined for traverses A and B and traverse C, and the mantle velocity is definitely subnormal (7.8 km/sec).

The travel-time plot for Line E shows a significant difference in the crustal velocity structure from that at site D. The mantle velocity at E (7.3 km/sec) is even more subnormal than that on Line D. There is some question as to whether the 7.3 km/sec layer actually represents mantle material or even a separate deep crustal layer, as there is an apparent time offset in the first arrivals on the eastern half of this traverse. The data could be interpreted as representing a change in dip for the 6.9 km/sec layer on crossing a fault. However, since the arrivals (admittedly weak evidence in this case) on the west leg of the profile support the interpretations of a low-velocity mantle, the latter interpretation was adopted. Figure 7 shows the derived crustal sections for the two sites.

LINES F AND G: The travel-time plots for Lines F and G are shown in Figure 9. Here, in Line F, as at site E, the mantle has a subnormal velocity (7.5 km/sec) which is well established by first arrivals in both directions from the recording site. The velocity structure of the crust (Fig. 8) is similar to that for site D, but the thickness of the crust and depth of the mantle (8 km) is markedly less, although the water depth is essentially the same.

In Line G, although the reversed values satisfactorily define the velocity structure of the crust, the mantle velocity was defined in only one direction. Figure 8 shows the derived crustal sections for sites F and G.

TABLE 2

VELOCITY AND TIME-INTERCEPT DATA FROM TRAVEL-TIME PLOTS

		VELOCITY (km/sec)						TIME INTERCEPT (seconds)					
STATION		SEDIMENTS	LAYER a	LAYER b	LAYER c	LAYER d	MANTLE	SEDIMENTS	LAYER a	LAYER b	LAYER c	LAYER d	MANTLE
A			4.62	5.58	6.21		7.96		5.3	5.7	6.25		10.44
A*		2.31	3.75	5.14	6.19		8.04	2.9	4.0	4.4	5.75		9.3
B		2.08		4.65	6.3			1.8		3.35	5.6		
B*		1.93		5.0	6.3		8.1	1.1		2.8	3.9		8.9
C		2.22	3.6	5.0	6.3	7.1	8.5	3.0	4.6	5.2	5.93	7.0	9.4
C*		2.05	3.5	4.95	5.78	7.0		3.6	5.5	6.35	6.9	8.0	
D	W	2.9		4.56		6.56	7.6	4.8		6.0		6.8	9.2
D	E	2.9		4.5		6.68	8.0	4.8		6.0		6.8	9.2
E	SW	(2.8)	4.08		6.15	6.98			2.0		2.85	3.6	
E	NE	(2.8)	4.05		5.8	6.75	7.28		2.0		2.85	3.8	5.18
F	W	2.52		4.4	6.12		7.43	4.26		5.4	6.0		6.4
F	E	2.52		4.47	6.78		7.61	4.26		5.4	6.0		6.4
G	SW		3.0	5.63		6.45	7.9		3.85	4.65		4.95	6.0
G	NE		3.0	5.1		6.75			3.85	4.81		5.42	
I	SW	2.25	3.8	5.5		6.3	7.9	4.18	5.48	6.29		6.68	8.12
I	NE	2.30	3.9	5.8		6.63	8.1	5.34	6.58	7.48		7.8	8.55
J		2.37	3.6	4.9		6.7	7.5	5.4	6.4	7.1		7.7	8.3
K	SW	2.25	3.74	5.0		6.42	7.6	4.62	5.64	6.19		6.78	7.83
K	NE	2.32	3.5	5.0		6.6	7.83	5.23	6.31	6.77		7.71	8.65
M	W		3.91	5.36		6.62	8.0		9.95	10.9		11.7	13.03
M	E		3.48			6.7	7.8		9.95			12.4	13.03
P	W	2.0	3.1	5.06		7.33	8.29	1.5	3.2	4.47		5.55	6.39
P	E	2.0	3.0	4.83		6.72	7.8	0.6	2.3	3.4		4.03	5.4

TABLE 3

Seismic Crustal Parameters, Solomon Islands Region

Station		Velocity (km/sec)						Thickness (km)						Depth to Mantle (km)
		Sediments	Layer a	Layer b	Layer c	Layer d	Mantle	Water	Sediments	Layer a	Layer b	Layer c	Layer d	
A		2.3	4.1	5.3	6.2		8.0	4.7	0	0.3	2.3	19.4		26.7
A*		2.3	4.1	5.3	6.2		8.0		0.8	0.2	6.7	14.3		25.0
B		2.0		4.8	6.3			2.1	0.8		8.1			
B*		2.0		4.8	6.3		8.1	1.3	1.3		3.8	23.5		29.9†
C		2.1	3.5	5.0	6.0	7.0	8.5	3.2	1.0	0.8	2.6	4.9	13.0	25.5†
C*		2.1	3.5	5.0	6.0	7.0		3.8	1.2	1.3	1.6	5.3		
D		2.9		4.5		6.6	7.8	4.2	1.3		1.6		14.3	21.4
E		2.8	4.1		6.0	6.9	7.3	1.4	0.4	2.0		4.6	13.4	21.8††
F		2.5		4.4	6.4		7.5	4.0	0.6		1.2	2.0		7.8
G	SW		3.0	5.3		6.6	7.9	3.3		0.7	1.0		5.6	10.6†††
G	NE		3.0	5.3		6.6		3.3		1.0	2.3			
I	SW	2.3	3.8	5.6		6.5	8.0	4.2	0.5	1.3	1.6		6.5	14.1
I	NE	2.3	3.8	5.6		6.5	8.0	5.3	0.1	1.5	1.2		2.3	10.4
J		2.4	3.6	4.9		6.7	7.7	5.4	0.4	0.5	1.3		3.6	11.2
K	SW	2.3	3.6	5.0		6.5	7.7	4.6	0.1	0.7	1.6		5.6	12.6
K	NE	2.3	3.6	5.0		6.5	7.7	5.2	0.1	0.4	3.0		4.6	13.3
M	W		3.9	5.4		6.6	8.0	8.3		1.6	2.4		6.7	19.0
M	E		3.5	5.4		6.7	7.8	8.5		0.7	6.0		1.7	16.9
P	W	2.0	3.1	4.9		7.0	8.0	1.7	1.5	1.6	2.9		5.0	12.7
P	E	2.0	3.1	4.9		7.0	8.0	0.7	1.9	1.4	1.5		9.2	14.7

† Mantle velocities and depths from weak data, generally later arrivals. Depths should be considered minimums.
†† The 7.3 km/sec velocity observed here may be a structural effect such as a normal fault with the raised side nearer the receiving vessel.
††† Mantle arrival unreversed.

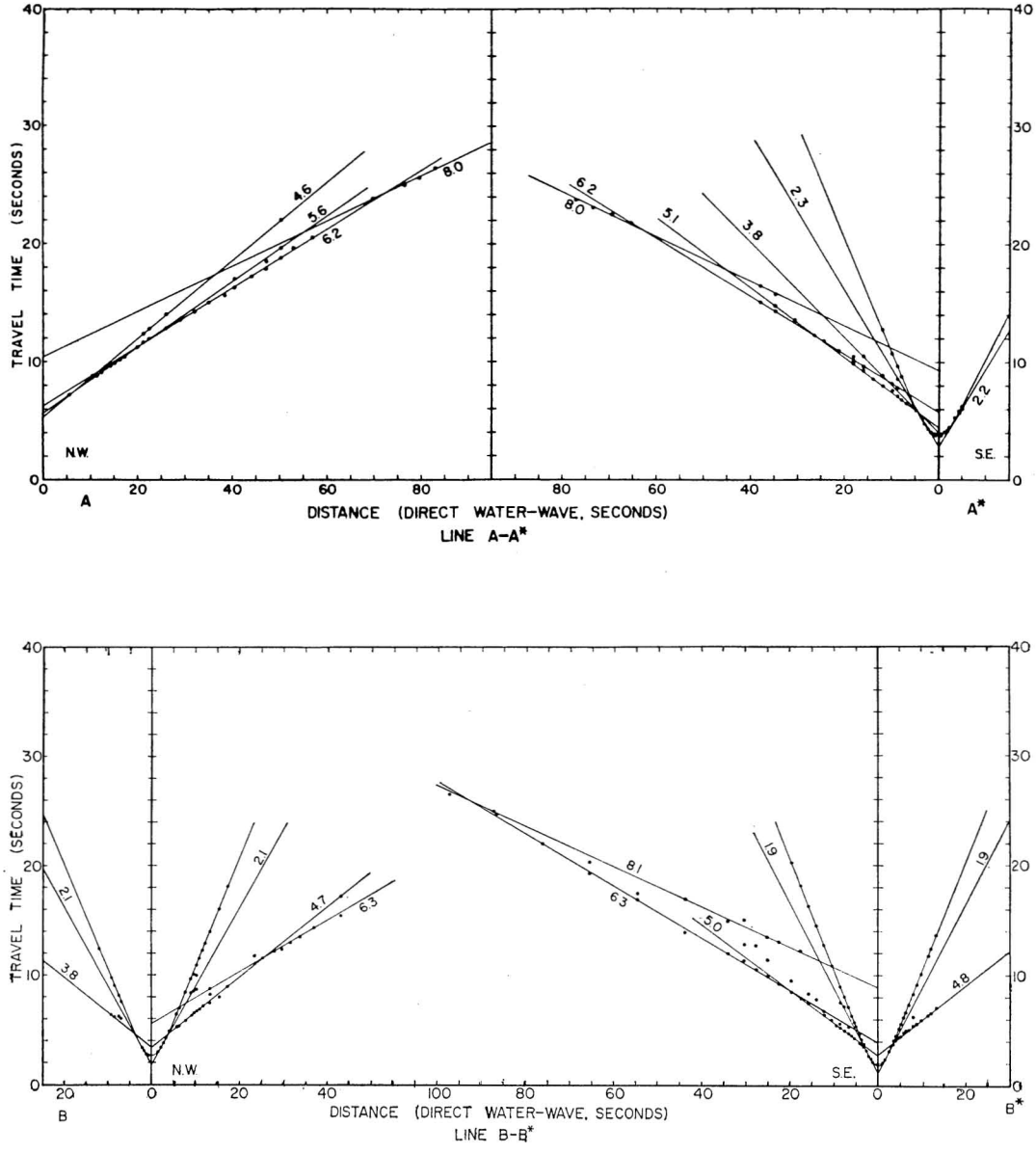

FIG. 3. Travel-time plots of Lines A–A* and B–B*. The velocity values of the various branches are in km/sec.

LINES I, J, AND K: The travel-time plots for Lines I, J, and K are shown in Figure 10. Few second arrivals could be identified, and the velocity values are not as well defined for the northeastern series of observations as for the southwestern series. By using reciprocal travel times between the two recording sites, however, true velocity values could be determined.

In Line J, good first arrivals were obtained only for the northwestern series of observations, and so the line was solved as a single-ended profile. The interpretation fits fairly well with the reversed profile interpretations from I and K. A check on the validity of the depths defined for the southeastern end of Line J—obtained by assuming horizontal layers from the northwest-

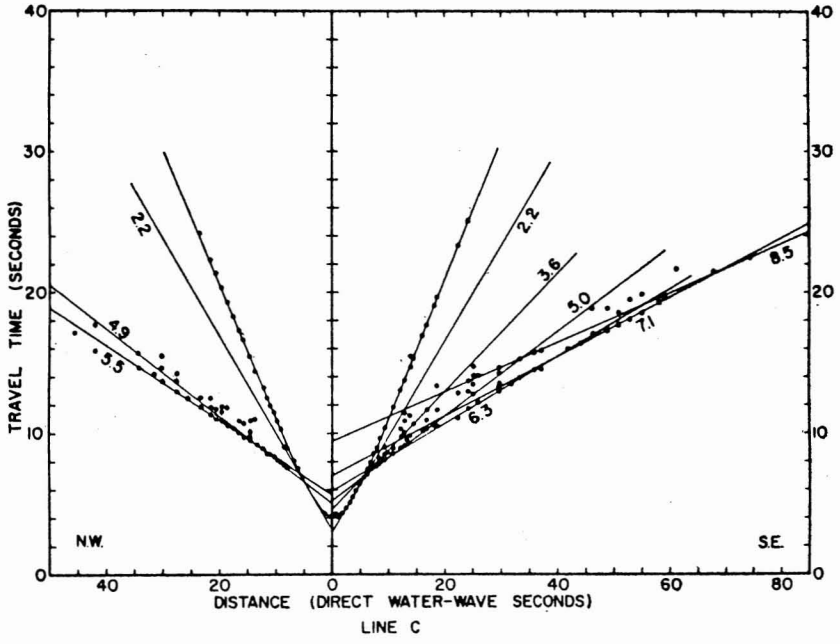

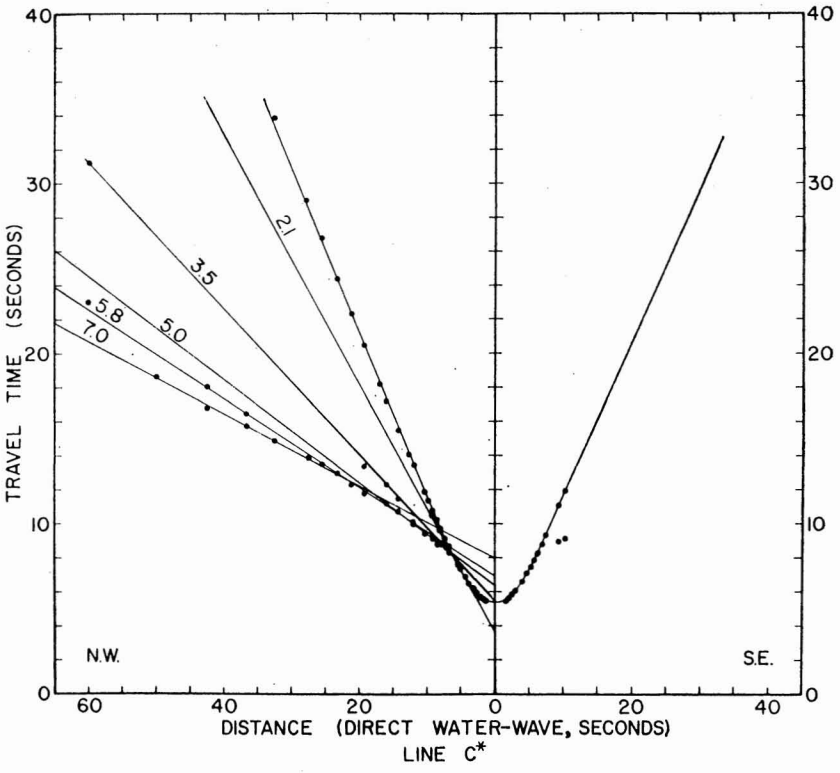

FIG. 4. Travel-time plots for Lines C and C*.

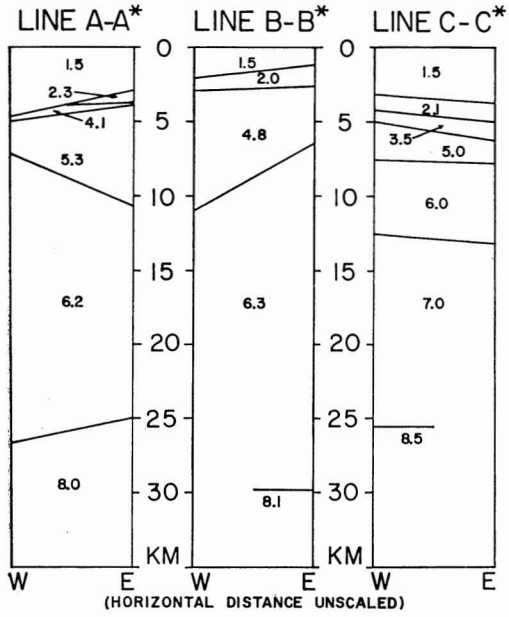

FIG. 5. Structural sections for Lines A–A*, B–B*, and C–C*. Velocity values are in km/sec; depths are in kilometers.

ern end interpretation—is possible, since the southeastern end of the line is almost coincident with the northeastern end of Line I. The depths to the various layers and to the Moho are in reasonable agreement. As similar depths were obtained using time-intercept values from the northeastern end of Line I to reverse Line J, the accuracy of the single-ended interpretation appears to be substantiated.

While there is some question as to the exact value for the mantle velocity of Line J, there is no question that the value is markedly subnormal (approximately 7.7 km/sec).

For Line K, the crustal velocity structure defined (Fig. 11) is similar to that found on Lines I and J. The mantle velocity on Line K is also subnormal.

A composite crustal section based on Lines I, J, and K is shown in Figure 11. On the whole, the depth to the mantle is rather uniform for this region, varying from 11.5 km to 14 km, and the variation in the velocity and thickness of the various crustal layers is small. The thickest layer is the basal layer, which has a velocity of 6.5 km/sec, and, except for subnormal mantle velocity values, the relations are similar to those generally found in the open ocean.

LINES M AND P: The travel-time plots for Lines M and P are shown in Figure 13. In Line M, mantle velocity is defined only for the eastern series of observations, but it is possible, using the intercept value and the time for the farthest first arrival on the western series of values, to define a mantle-velocity value of 8.0 km/sec for the western series. As the travel-time plots for the eastern and western series are markedly different, in terms of both velocity values and intercept values, it is possible that the recording vessel was located over a fault. The data for the two series of observations were therefore studied separately and independent solutions obtained for the crustal structure on the assumption of horizontal layers. This assumption is justified as the profiles were oriented along the geologic strike. In deriving the structure for the eastern series of observations, a 5.4 km/sec layer was arbitrarily introduced in the data analysis in order to obtain agreement in number of layers present on the two sides of the hypothetical fault. The derived crustal structure under Line M using the eastern and western series of observations is shown in Figure 12.

In Line P, very good arrivals were obtained for all ranges on this profile and there is no question regarding the velocity of the mantle, which is slightly subnormal (8.0 km/sec). The structural section is shown in Figure 12.

Recapitulation of Results

As discussed in the previous section, in connection with the individual travel-time plots, the velocity values for the crustal layers on all of the traverses were well established except on lines M, I, and J. The greatest uncertainty in the thickness values for the crust at the various sites is related to the use of split profiles for Lines D, E, F, and M and the failure to obtain reverse velocity values for the mantle on Lines B, C, E, J, and G. The probable error in overall crustal thickness for these sites is of the order of $\pm$ 10 to 15 percent. For the other sites, the estimated error is less than 10 percent. These estimates are based on trial calculations for models having parameters comparable to those observed at the sites. In no case is it felt that the crustal thickness is as much as 20 percent in error. The marked regional differences in the thickness of the crust, with mantle depth vary-

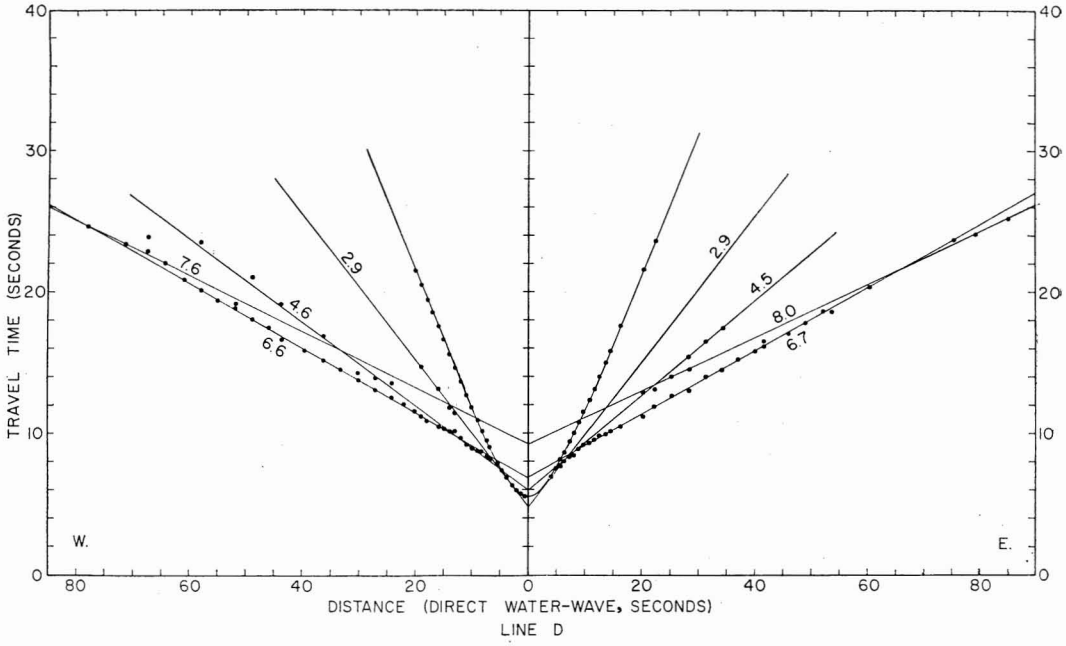

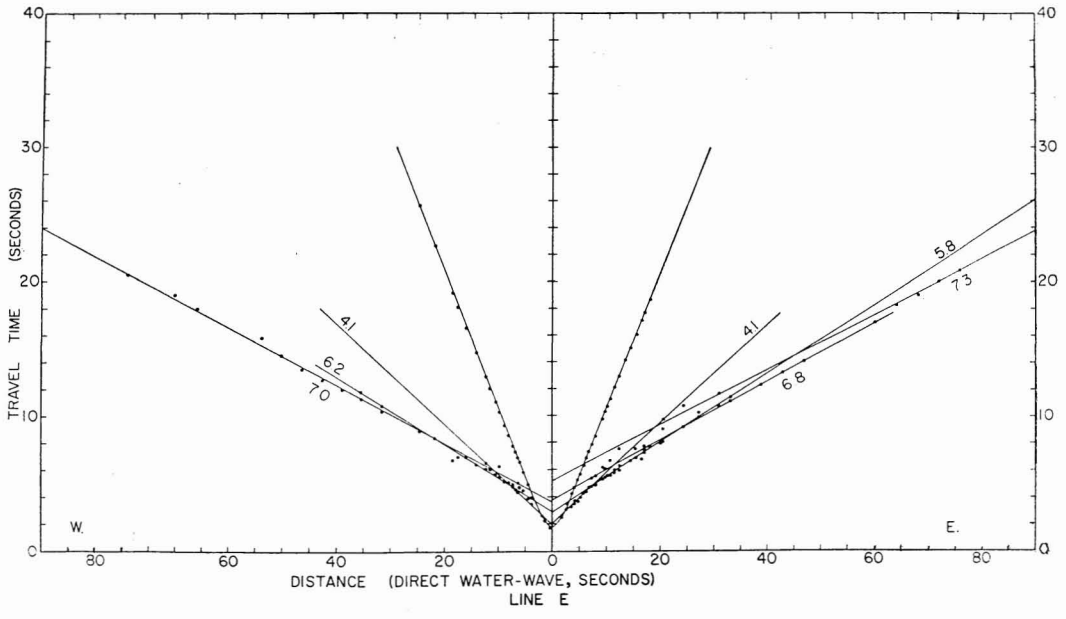

FIG. 6. Travel-time plots for Lines D and E.

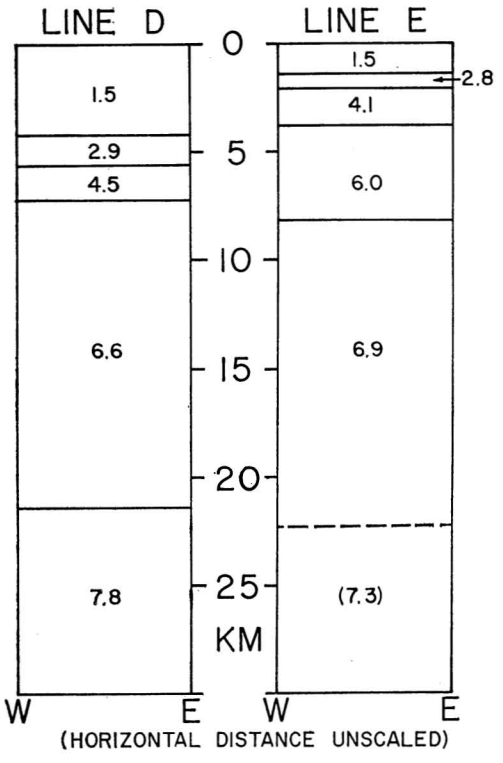

FIG. 7. Structural sections for Lines D and E. Velocity values are in km/sec; depths are in kilometers.

ing from 8 km to over 25 km below sea level, are therefore real and not a product of weak data.

Relationships Brought Out by the Data

Simplified structural sections have been plotted in Figure 14 on a map of the Solomon Islands region to give a composite picture of crustal and upper-mantle relations in the area. Also shown in the figure is a crustal section for the island of New Britain based on data from the Rabaul Seismic Experiment conducted in 1967 with the Bureau of Mineral Resources, Commonwealth of Australia. This crustal section of New Britain Island is based on a preliminary interpretation of that portion of the data taken by the writers as part of a cooperative effort with the Bureau of Mineral Resources and is subject to modification upon completion of the program.

CONCLUSIONS

The crustal refraction work around the Solomon Islands has indicated the following three generalized crustal regions:

(1) Northwest of Malaita and Santa Isabel on the Ontong Java Plateau, where mantle depths of 20 to 25 km were observed with normal mantle velocities, but where crustal velocities are subnormal (6.0 to 6.3 km/sec) for the most part.

(2) Southwest of New Georgia Island, where a subnormal crustal thickness and mantle velocity are found.

(3) Southwest of Bougainville Island, where generally "normal" oceanic structure is found, although the upper mantle velocity is subnormal.

These regions can also be identified by distinctly different gravity anomaly patterns. The first area has a subnormal gravity field; the

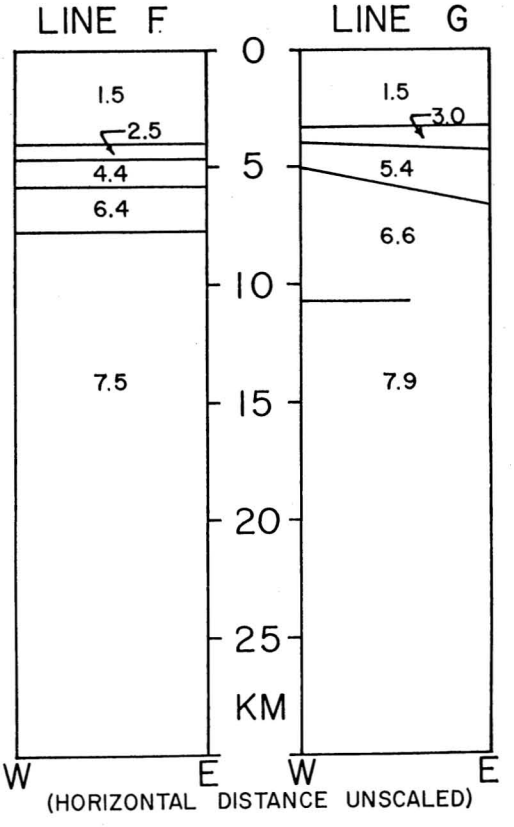

FIG. 8. Structural sections for Lines F and G.

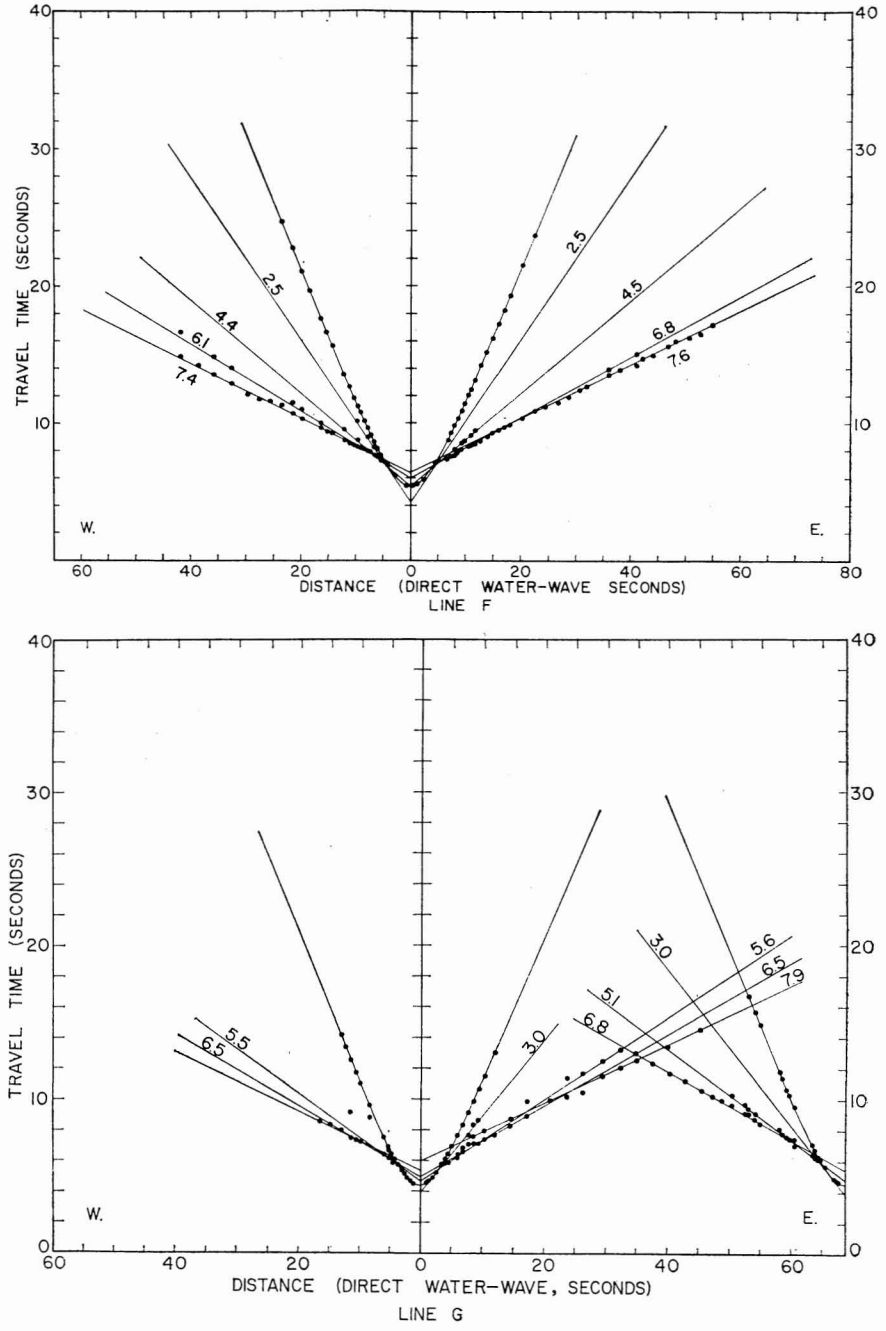

FIG. 9. Travel-time plots for Lines F and G.

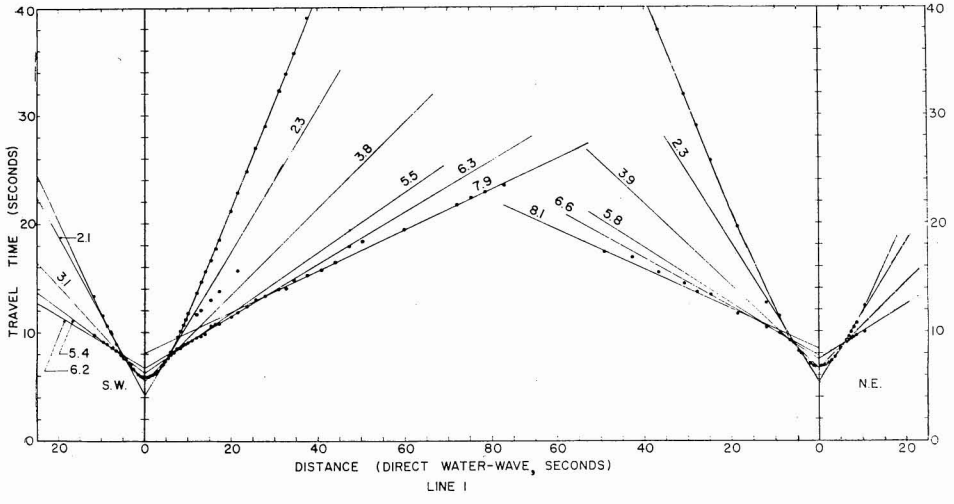

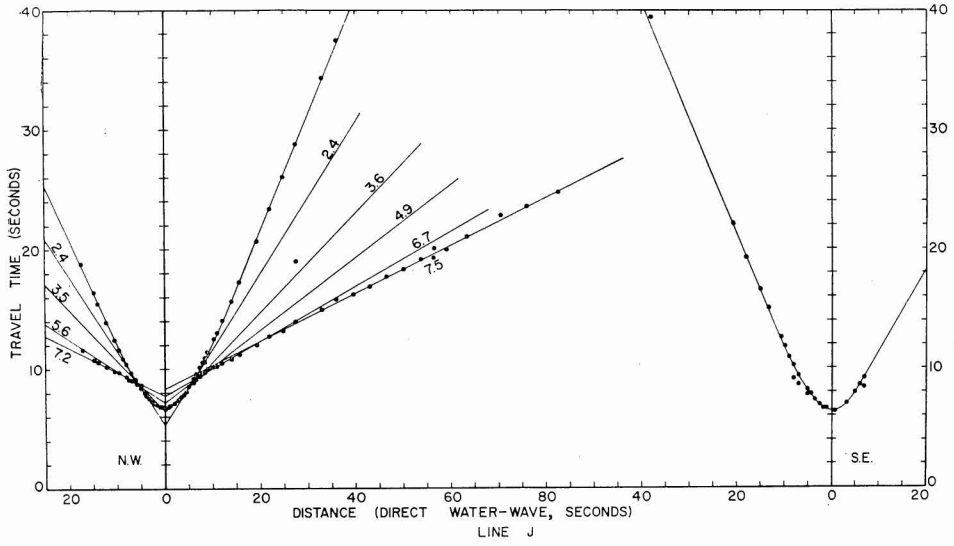

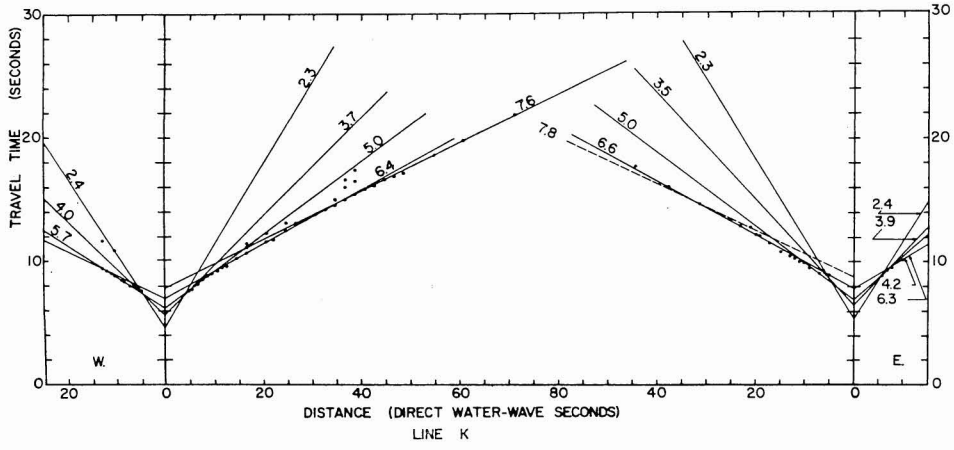

FIG. 10. Travel-time plots for Lines I, J, and K.

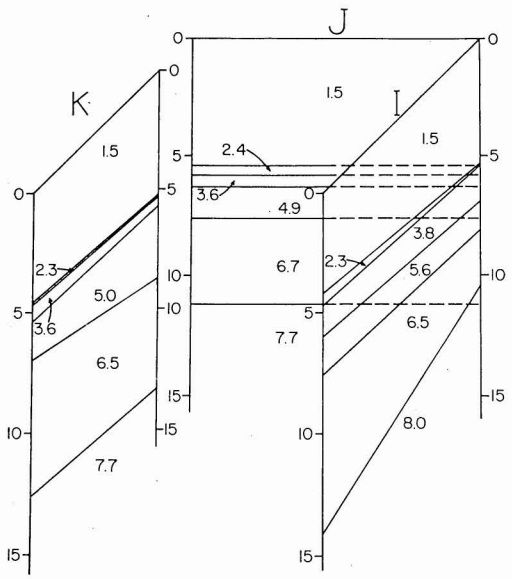

FIG. 11. A three-dimensional representation of crustal sections for Lines I, J, and K.

second, a near-normal gravity field; and the third, a characteristic abnormal gravity field (free-air anomalies of +100 mgal).

At Line P in the Slot, the mantle lies at a depth of about 14 km, intermediate between the first and second areas. Gravity calculations for this shallow-water area (less than 1.5 km) would indicate a free-air anomaly of up to +200 mgal for the seismically observed crustal structure, yet the observed gravity anomaly is zero to slightly negative. It is in this region that proponents of the "new global tectonics" predict a convergence zone between two conjectured plates, one from the Pacific moving from the north and east, and the other from the Coral Sea moving from the southwest. From present data, one suggested hypothesis is that the Coral Sea plate is being thrust under the Pacific plate. This hypothesis is based on the following observations:

(1) The area of maximum crustal thickness is not under the Solomon Islands, but is to the north under the Ontong Java Plateau.

(2) Continuous seismic reflection profiles (Woollard et al., 1967) indicate that the northern boundary of the Solomon Platform is a high-angle thrust fault and that the broad anticlinal arch seaward of this feature is the result of crustal shortening. It is over this area that Line B shows a crustal thickness of nearly 30 km, possibly the result of the thrusting of the one plate under the other to effectively double the crustal thickness.

Other suggestions are possible and the authors are presently engaged in testing them.

ACKNOWLEDGMENTS

The authors wish to express their gratitude to Mr. John C. Grover, former Chief of the Geological Survey, British Solomon Islands Protectorate, for his generous and unstinting cooperation while the project was underway. We also wish to thank the staff members of the Geological Survey and of the various agencies of the British Solomon Islands Protectorate for assisting in ship preparations at Honiara. We

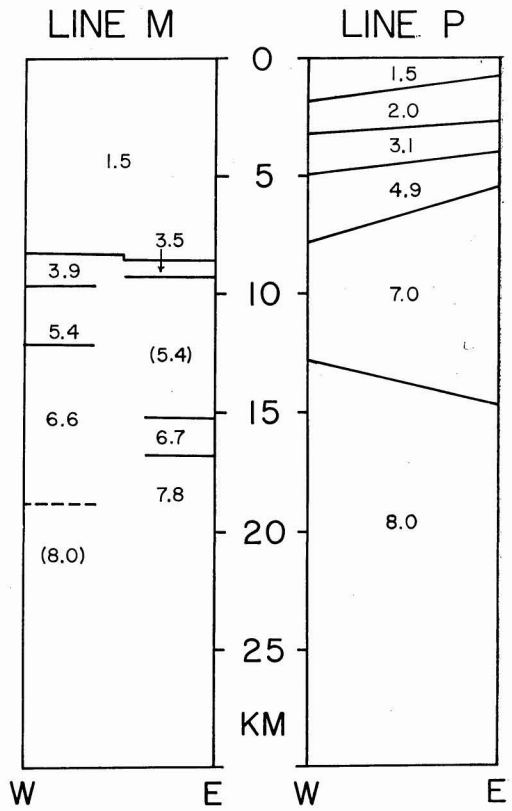

FIG. 12. Structural sections for Lines M and P. Velocity values are in km/sec; depths are in kilometers. Values in parentheses are assumed values.

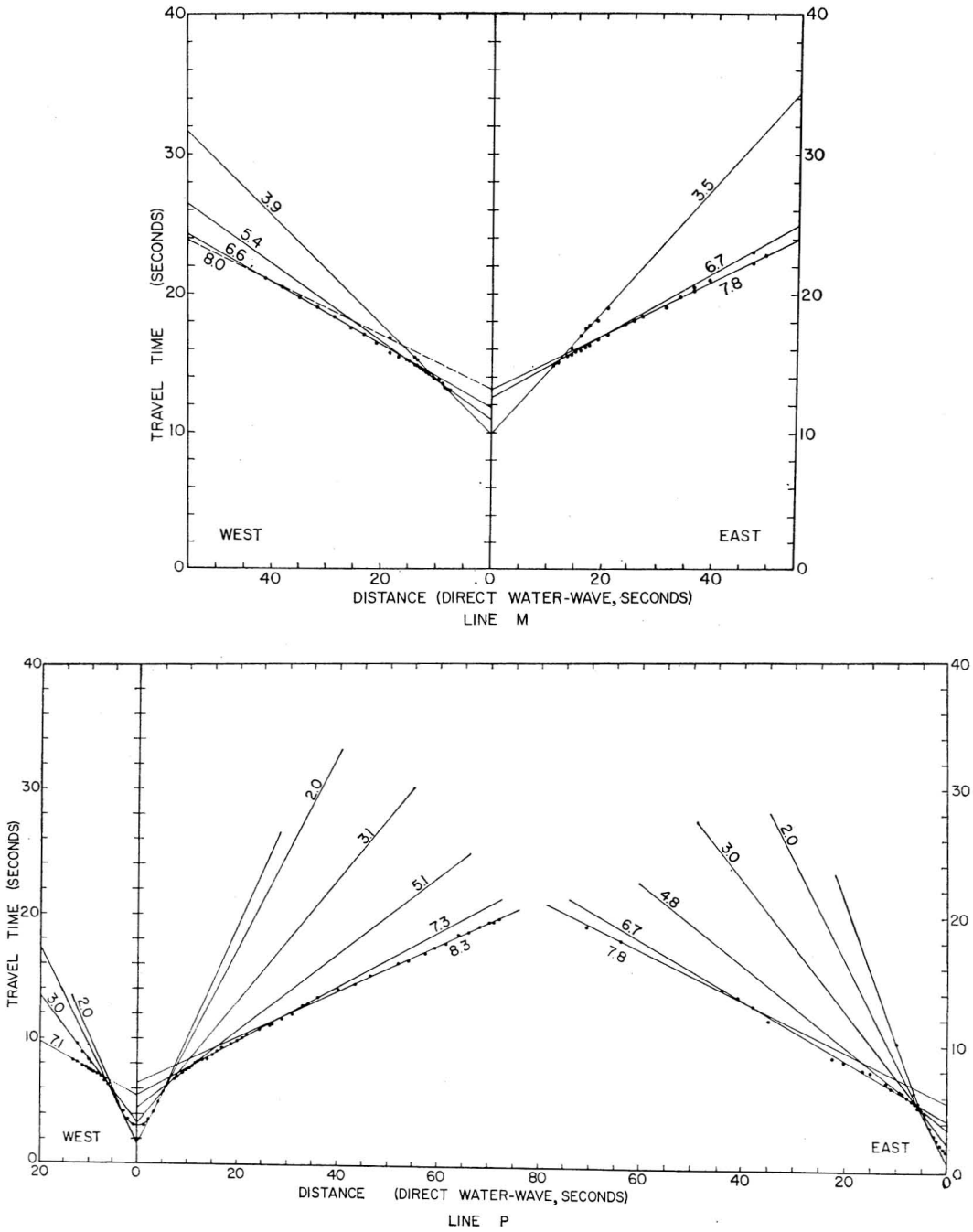

FIG. 13. Travel-time plots for Lines M and P.

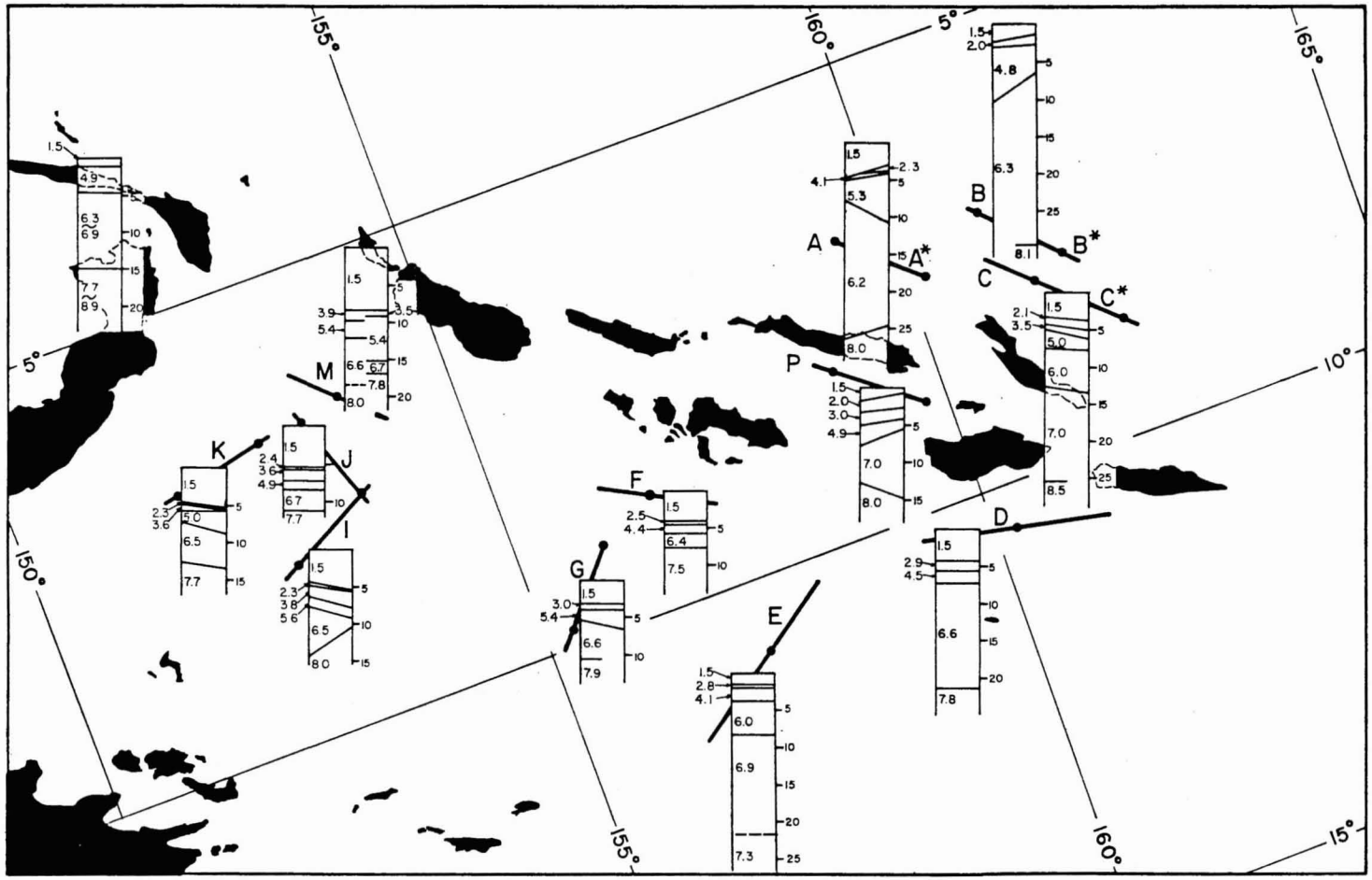

Fig. 14. Composite crustal and upper mantle structure of the Solomon Islands and Bismarck Archipelago. Velocity values are in km/sec; depths are in kilometers.

wish to acknowledge the contribution of the following men during the work at sea: Dr. Gary Stice, William Ichinose, Jr., Ed Houlton, David Schlabach, Ted Murphy, Robert Harvey, Kelly Blackburn, Loren Kroenke, Donald Klim, Herbert Rosenbusch, and Robin Zachariadis.

We are also grateful for the understanding and cooperation of officers and men of the SS "Taranui," the RV "California," and the RV "Machias" in carrying out the project.

The field work was supported by Office of Naval Research contract NONR 3748(05) and the analysis was partially supported by National Science Foundation grants GP 5111 and GA 1084.

LITERATURE CITED

GROVER, J. C. 1968. The British Solomon Islands: Some geological implications of the gravity data, 1966. In: Leon Knopoff, Charles L. Drake, and Pembroke J. Hart, eds., The crust and upper mantle of the Pacific area, pp. 296–306. Geophysical Monograph 12, American Geophysical Union, Washington, D. C.

LAUDON, T. S. 1968. Land gravity survey of the Solomon and Bismarck Islands. In: Leon Knopoff, Charles L. Drake, and Pembroke J. Hart, eds., The crust and upper mantle of the Pacific area, pp. 279–295. Geophysical Monograph 12, American Geophysical Union, Washington, D. C.

ROSE, J. C., G. P. WOOLLARD, and A. MALAHOFF. 1968. Marine gravity and magnetic studies of the Solomon Islands. In: Leon Knopoff, Charles L. Drake, and Pembroke J. Hart, eds., The crust and upper mantle of the Pacific area, pp. 379–410. Geophysical Monograph 12, American Geophysical Union, Washington, D. C.

SHOR, G. G., JR. 1963. Refraction and reflection techniques and procedure. In: M. N. Hill, ed., The sea: Ideas and observations. 1st ed. Vol. 3, pp. 20–38. New York, John Wiley and Sons.

SUTTON, G. H., and C. R. BENTLEY. 1953. Topographic correction curves. Lamont Geological Observatory Technical Report 3, 5 pp.

WOOLLARD, G. P. 1968. The interrelationship of the crust, the upper mantle and isostatic gravity anomalies in the United States. In: Leon Knopoff, Charles L. Drake, and Pembroke J. Hart, eds., The crust and upper mantle of the Pacific area, pp. 312–341. Geophysical Monograph 12, American Geophysical Union, Washington, D. C.

WOOLLARD, G. P., A. S. FURUMOTO, G. H. SUTTON, J. C. ROSE, A. MALAHOFF, and L. W. KROENKE. 1967. Cruise report on the 1966 seismic refraction expedition to the Solomon Sea. Hawaii Institute of Geophysics Report 67-3, 31 pp.